Analytical Expressions for Thermo-Osmotic Permeability of Clays

J. Goncalves, C. Ji Yu, Jean Michel Matray, Joachim Tremosa

AGU PUBLICATIONS

Geophysical Research Letters

RESEARCH LETTER
10.1002/2017GL075904

Key Points:
- Thermo-osmotic permeability for for clay-rocks with monovalent-divalent solutions is ascertained
- Based on limiting case analysis, analytical expressions for thermo-osmotic coefficients are proposed
- Introducing divalent cations only slightly weakens thermo-osmosis contrarily to chemo-osmosis

Supporting Information:
- Supporting Information S1

Correspondence to:
J. Gonçalvès,
goncalves@cerege.fr

Citation:
Goncalves, J., Yu, C. J., Matray, J.-M., & Tremosa, J. (2018). Analytical expressions for thermo-osmotic permeability of clays. *Geophysical Research Letters, 45,* 691–698. https://doi.org/10.1002/2017GL075904

Received 2 OCT 2017
Accepted 2 JAN 2018
Accepted article online 8 JAN 2018
Published online 24 JAN 2018

Analytical Expressions for Thermo-Osmotic Permeability of Clays

J. Gonçalvès[1], C. Ji Yu[2], J.-M. Matray[2], and J. Tremosa[3]

[1] Aix-Marseille Université, CNRS, IRD, Collège de France, CEREGE, Aix-en-Provence, France, [2]IRSN, Institut de Radioprotection et de Sureté Nucléaire, Fontenay-aux-Roses, France, [3]BRGM, Bureau de Recherches Géologiques et Minières, Orléans, France

Abstract In this study, a new formulation for the thermo-osmotic permeability of natural pore solutions containing monovalent and divalent cations is proposed. The mathematical formulation proposed here is based on the theoretical framework supporting thermo-osmosis which relies on water structure alteration in the pore space of surface-charged materials caused by solid-fluid electrochemical interactions. The ionic content balancing the surface charge of clay minerals causes a disruption in the hydrogen bond network when more structured water is present at the clay surface. Analytical expressions based on our heuristic model are proposed and compared to the available data for NaCl solutions. It is shown that the introduction of divalent cations reduces the thermo-osmotic permeability by one third compared to the monovalent case. The analytical expressions provided here can be used to advantage for safety calculations in deep underground nuclear waste repositories.

1. Introduction

Among the osmotic processes known to occur in natural clay rocks, electro-osmosis (Revil & Pessel, 2002; Zhang & Wang, 2017) and especially chemical osmosis (Neuzil, 2000) have attracted most of the attention. The latter is well documented (see, e.g., Gonçalvès et al., 2015; Neuzil & Provost, 2009) with a particular focus on nuclear waste storage in deep geological formations. However, and despite the possible existence of natural (low thermal conductivity) or artificial (nuclear waste storage) elevated thermal gradients, thermo-osmosis, a fluid flow driven by a temperature gradient has not received the same attention. One reason is that the theoretical framework for thermo-osmosis is less comprehensive than that for chemical osmosis. Nevertheless, the physical basis of thermo-osmosis, at the molecular and pore scales, was established in the early twentieth century by Derjaguin and coworkers (Churaev, 2000; Derjaguin & Sidorenkov, 1941) within the framework of irreversible thermodynamics. When a pressure gradient is prescribed through a porous membrane at initial constant temperature, the fluid flow causes a temperature gradient buildup (see Figure 1), the so-called mechanocaloric effect. The related heat flux is attributed to a specific enthalpy of the pore fluid which differs, at the pore scale, by a quantity Δh (J m^{-3}) from that of the bulk fluid (Churaev, 2000; Derjaguin & Sidorenkov, 1941). Note that the bulk solution can be theoretically found in adjacent aquifers or in macropores not subjected to any electrical field. This difference Δh is caused by the alteration of the hydrogen bond (HB) network and energy of the water molecules due to fluid-mineral electrical interactions (Churaev, 2000). In the event of hydrogen bonding weakening (HB concentration decreases), heat adsorption at the inlet of pore space and heat release at the outlet causes the temperature gradients shown in Figure 1 (Churaev, 2000). According to Onsager's reciprocity principle, the counterpart of the mechanocaloric effect, that is, thermo-osmosis, must exist and thus relies on the same physical basis, that is, pore water structure alteration. Since such a thermo-osmotic process has been observed in clay-rich materials (see, e.g., Tremosa et al., 2010), the possible occurrence and causes of HB alteration in the pore space of clay rocks must be analyzed. The negative surface charge of clay minerals at natural pH is balanced by counterions (cations, Mitchell, 1993; Sposito et al., 1999) forming with the mineral surface the electrical double layer. However, solvated ions cause a disruption of HB particularly in the first hydration shells. Therefore, while the average number of HB is 3.5 for bulk water molecules, it is 2.27 in the first hydration shell of Na^+ (Guàrdia et al., 2005). Conversely, highly structured (strongly hydrogen bonded) water molecules in the close vicinity of clay mineral surface have been documented (Mitchell, 1993). This is supported by molecular dynamics simulations showing a water structure

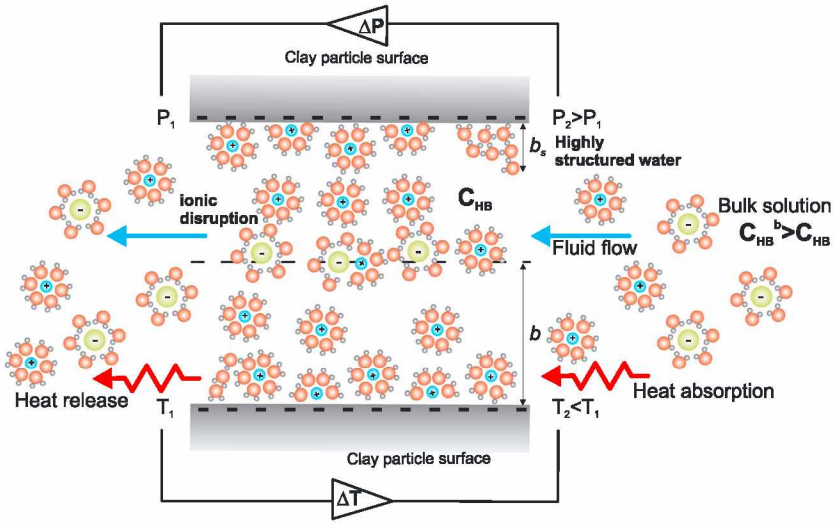

Figure 1. Schematic view of the average representative pore (see supporting information for geometrical conceptualization) and clay surface-pore fluid interactions reproduced from Gonçalvès et al. (2012, Figure 1). In blue and green, the cations and the anions with their first solvation shell; in red and grey, water molecules. C^b_{HB} and C_{HB} are the hydrogen bond (HB) concentrations in the bulk solution and in the pore fluid, b and b_s the half interparticle distance and half-thickness of highly structured water. Δp and ΔT are the pressure and temperature gradients. When a pressure gradient Δp is instantaneously imposed, heat absorption (breaking of HB) occurs when fluid enters the pore if $C^b_{HB} > C_{HB}$ due to solid-fluid interactions. Conversely, heat is released at the outlet which causes the temperature gradient ΔT defining the so-called mechanocaloric effect. A thermo-osmotic flow can then balance the Darcy flow and an equilibrium is attained ($q = 0$; see equation (1)).

evolving from an almost ice-like (4 HB) first monolayer of water at the mineral surface toward a roughly bulk water structure in the third layer (3.5 HB) at about 1 nm distance (Kirkpatrick et al., 2005; Marry et al., 2008).

The second reason for an apparently lower interest in thermo-osmosis in natural media is doubtless the absence of a practical-use model for thermo-osmotic permeability. Although some substantial improvements can be expected regarding the fundamental physical chemistry supporting thermo-osmosis, the available molecular-based theoretical background can be conveniently used to obtain a desirable macroscopic law for practical thermo-osmosis calculations in geological media. In a first step, we used a simple volume-averaging approach (upscaling) to obtain a macroscopic transport coefficient from a microscopic analysis which yields (Gonçalvès & Tremosa, 2010)

$$q = -\frac{k}{\eta}(\nabla p + \rho g \nabla z) - \frac{k\Delta H}{\eta T}\nabla T, \tag{1}$$

where q is the pore fluid-specific discharge (m s^{-1}), k is the Darcy permeability (m^2), η is the dynamic viscosity (Pa s), p is the pressure (Pa), ρ is the fluid density (kg m^3), g is the acceleration due to gravity (m s^{-2}), ∇z is (0,0,1) if the z axis is vertical upward, T is the temperature (K), and ΔH is the macroscopic volume-averaged excess specific enthalpy due to fluid-solid interactions (J m^{-3}). According to equation (1), the thermo-osmotic permeability is $k_T = k\Delta H/T$ (Pa m^2 K^{-1}). Most often, $\Delta H > 0$ in clays, and fluid flow occurs in the direction of decreasing temperature, but negative values have also been reported (see, e.g., Tremosa et al., 2010).

In a heuristic approach, we directly formalized the enthalpy change ΔH due to hydrogen bonding modifications at the macroscale to obtain a theoretical expression for the thermo-osmotic coefficient $\varepsilon_T = k_T/k$ for clays in purely monovalent solutions (Gonçalvès et al., 2012). However, addressing such process in natural media requires accounting for two major characteristics of shale formations: (i) the heterogeneity of the material with the presence of additional solid phases (carbonate and sand) besides the clay fraction and (ii) the likely presence of divalent cations such as Ca^{2+} (Tremosa et al., 2012). The presence, even at a low concentration, of divalent cations can be explained by the existence of even relatively small amounts of carbonate in the shale formation, fluid clay minerals interactions, or by vertical leakage from adjacent carbonate aquifers. Therefore, here it is proposed to extend the previous work by Gonçalvès et al. (2012) to monovalent-divalent pore fluid solutions allowing a relevant discussion for natural media. In addition, this study presents a more

comprehensive discussion of controlling parameters for k_T as well as providing convenient analytical expressions not available to date in the literature. In addition, the manuscript discusses the implications of taking into account the divalent cations that are naturally present in geological media.

2. Mathematical Formulation

The model is developed for a monovalent/divalent system which describes many natural Na-Ca-Cl solutions. According to the molecular-based theoretical framework outline above, more structured water at the clay mineral surface and the disruption of HB caused by the ionic content of solutions have to be formally described. HB disruption requires estimating the pore space average ionic content. The negative surface charge of clay minerals at natural pH is balanced by more concentrated cations (counterions), while anions (co-ions) are less concentrated than in the bulk solution. Similarly to the pure monovalent case (see, e.g., Revil & Leroy, 2004), ionic concentrations can be conveniently estimated using a simple Donnan equilibrium formalism for a monovalent-divalent system by equating the chemical potentials of the ions in the bulk solution:

$$\mu_+ = \mu_+^R + k_b T \ln c_+, \tag{2}$$

$$\mu_- = \mu_-^R + k_b T \ln c_-, \tag{3}$$

$$\mu_{2+} = \mu_{2+}^R + k_b T \ln c_{2+}, \tag{4}$$

to their counterpart, that is, the electrochemical potentials of the ions, in the pore space solution of a clay rock:

$$\overline{\mu_+} = \mu_+^R + k_b T \ln C_+ + e\varphi, \tag{5}$$

$$\overline{\mu_-} = \mu_-^R + k_b T \ln C_- - e\varphi, \tag{6}$$

$$\overline{\mu_{2+}} = \mu_{2+}^R + k_b T \ln C_{2+} + 2e\varphi, \tag{7}$$

where C_+, C_-, and C_{2+}, and c_+, c_-, and c_{2+} are the concentrations of monovalent cation, anion, and divalent cation in the pore space and in the bulk solution, respectively; μ_+^R, μ_-^R, and μ_{2+}^R are the corresponding potentials at a reference state (the same for bulk and pore solutions); k_b is the Boltzmann constant (1.38×10^{-23} J K^{-1}); φ is the electrical potential in the pore space; and e is the elementary charge (1.6×10^{-19} C). Note that pore concentrations and electrical potential refer to average values representative of the pore space, while these variables are spatially distributed and functions of the distance from the mineral surface. Assuming a thermodynamic equilibrium between the bulk and the pore fluid solutions, that is, $\overline{\mu_+} = \mu_+$, $\overline{\mu_{2+}} = \mu_{2+}$, and $\overline{\mu_-} = \mu_-$ yields

$$C_{2+}C_-^2 = c_{2+}c_-^2, \tag{8}$$

and

$$C_+C_- = c_+c_-. \tag{9}$$

In addition, the electroneutrality equation in the pore is written as follows:

$$2C_{2+} + C_+ = C_- + \frac{Q_V}{e}, \tag{10}$$

where Q_V is the excess charge per unit pore volume (C m^{-3}) to be compensated by counterions. Q_V is obtained by dividing the excess charge (C) in a unit volume of porous medium $(1-\omega)\rho_s$CEC$\times$ 96.3 by the associated fluid volume ω yielding (Revil & Leroy, 2004)

$$Q_V = \frac{(1-\omega)\rho_s \mathrm{CEC} \times 96.3}{\omega}, \tag{11}$$

where ω is the porosity, ρ_s is the density of the solid (kg m^{-3}), and CEC is the cation exchange capacity (meq g^{-1}). Introducing equations (8) and (9) into equation (10) yields

$$C_-^3 + \frac{Q_V}{e}C_-^2 - (c_+ + c_-)C_- - 2c_{2+}c_-^2 = 0 \tag{12}$$

Upon resolution of equation (12), only one out of the three roots applies to the problem.

Table 1
Parameters of the Thermo-Osmotic Coefficient

Parameter	Value
N_w^+ (-)	6.00
N_w^- (-)	6.00
N_w^{2+} (-)	8.00
N_{HB}^+ (-)	2.27
N_{HB}^- (-)	2.65
N_{HB}^{2+} (-)	1.80
ΔH_{HB}^a (kJ mol^{-1})	14.50
v_+ (m^3 mol^{-1})	23.80×10^{-6}
v_- (m^3 mol^{-1})	17.40×10^{-6}
v_{2+} (m^3 mol^{-1})	26.02×10^{-6}
v_w (m^3 mol^{-1})	18.00×10^{-6}
N_{HB}^b (-)	3.5
N_{HB}^s [a] (-)	3.75
b_s^a (m)	10^{-9}

[a]The average values in the plausible range from the literature (Hakem et al., 2007; Kirkpatrick et al., 2005; Marry et al., 2008).

An expression for the required ΔH value according to the thermodynamic interpretation by Derjaguin and Sidorenkov (1941) was heuristically obtained by Gonçalvès et al. (2012) and is written as follows:

$$\Delta H = (C_{HB}^b - C_{HB})\Delta H_{HB} \tag{13}$$

where C_{HB}^b and C_{HB} are the HB concentrations (mol m^{-3}) in the bulk and the pore fluid and ΔH_{HB} (kJ mol^{-1} of HB) is the energy needed to break one mole of HB. Estimated values of ΔH_{HB} between 6 and 23 kJ mol^{-1} are reported (Hakem et al., 2007). Let C_w and N_{HB} be the water concentration (mol m^{-3}) in the pore space and the mean number of hydrogen bonds per water molecule, respectively. Taking into account the 1/2 binding order (Hakem et al., 2007) of a HB (one HB shared by two water molecules), the HB concentration C_{HB} is $C_w 1/2N_{HB}$. Consequently, the hydrogen bond concentrations are calculated for a monovalent-divalent system with

$$\begin{aligned} C_{HB} = {} & N_w^+ C_+ 1/2N_{HB}^+ + N_w^{2+} C_{2+} 1/2N_{HB}^{2+} + N_w^- C_- 1/2N_{HB}^- \\ & + (C_w - N_w^+ C_+ - N_w^{2+} C_{2+} - N_w^- C_-)\left(\frac{b-b_s}{b} N_{HB}^b + \frac{b_s}{b} N_{HB}^s\right) 1/2, \end{aligned} \tag{14}$$

and

$$\begin{aligned} C_{HB}^b = {} & N_w^+ c_+ 1/2N_{HB}^+ + N_w^{2+} c_{2+} 1/2N_{HB}^{2+} + N_w^- c_b 1/2N_{HB}^- \\ & + (c_w - N_w^+ c_+ - N_w^{2+} c_{2+} - N_w^- c_b) N_{HB}^b 1/2, \end{aligned} \tag{15}$$

where C_w, C_+, C_{2+}, and C_- are the water, monovalent and divalent cations, and anion concentrations (mol m^{-3}) in the pore space; c_w is the water concentration in the bulk solution; N_w^+, N_w^{2+}, and N_w^- are the number of water molecules in the first hydration shell of the monovalent and divalent cations and of the anion; N_{HB}^+, N_{HB}^{2+}, and N_{HB}^- are the mean number of HB per water molecule in the first corresponding hydration shells; b and b_s are the mean half pore size and the half thickness of highly ordered water (m); and N_{HB}^b and N_{HB}^s are the mean number of HB per water molecule of bulk and highly ordered water. The sum of the first three terms on the right-hand side of equation (14) is the number of HB per unit volume of pore fluid affected by ionic disruption, while the third term is the complementary part for water molecules outside the influence of ions. For the latter, $\frac{b-b_s}{b} N_{HB}^b + \frac{b_s}{b} N_{HB}^s$ represents the mean number of HB per water molecule accounting for the highly ordered water at the solid surface. The half pore size b can be calculated by equating $A_s b$ (m^3 kg^1 of solid) with A_s (m^2 g^{-1}) the specific surface area (SSA) to the water content per kg of solid $\omega/(1-\omega)\rho_s$ considering a plane-parallel conceptual geometry for the porous medium (Neuzil, 2000) yielding

$$b = \frac{\omega}{(1-\omega)\rho_s A_s}. \tag{16}$$

Note that introducing equation (16) into equation (11) yields $Q_V = \text{CEC} \times 96.3/A_s b = \sigma/b$, where $\sigma = \text{CEC} \times 96.3/A_s$ (C m^{-2}) is the solid surface charge density. The plane-parallel conceptualization for pores even for natural clay rocks is supported by mineralogical observations (see, e.g., Bennett & Hulbert, 1986; Leu et al., 2016; Wenk et al., 2008, and the supporting information). The HB concentration in the bulk solution (equation (15)) was obtained by setting $C_+ = c_+$, $C_{2+} = c_{2+}$, $C_- = c_b$, and b_s=0 in equation (14).

C_w and c_w are calculated using the mass conservation equations (see, e.g., Gonçalvès & Rousseau-Gueutin, 2008; Revil & Leroy, 2004):

$$v_w C_w + v_+ C_+ + v_{2+} C_{2+} + v_- C_- = 1 \tag{17}$$

and

$$v_w c_w + v_+ c_+ + v_{2+} c_{2+} + v_- c_b = 1, \tag{18}$$

where v_w, v_+, v_{2+}, and v_- are the molar volumes of the water, monovalent and divalent cations, and anion, respectively.

Upon resolution of equation (10), equations (8)–(18) form a model the main inputs for which are petrophysical parameters commonly measured in clay rocks together with molecular parameters that can be constrained

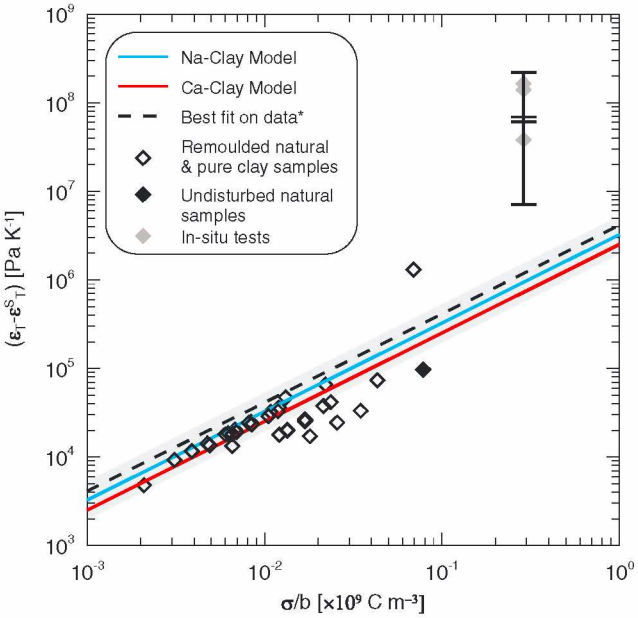

Figure 2. Available data (see Table S1 and details in the supporting information) for Clays in Na solutions (Al-Bazali, 2005; Cary, 1966; Dirksen, 1969; Gray, 1966; Habib & Soeiro, 1957; Rosanne et al., 2006; Taylor & Cary, 1960; Tremosa et al., 2010; Zheng & Samper, 2008) and model fitting curves obtained by multiple random simulations using the mathematical formulation proposed here (see text). For the data, b and σ were calculated using equations (16) and (11) together with their petrophysical parameters (ω, CEC, and A_S) listed in Table S1 in the supporting information, ε_T^S was calculated by introducing the b values into equation (21) and ε_T measurements were used. Natural stands for heterogeneous materials containing a nonclay minerals fraction. Error bars are only available for the in situ data and are associated with the uncertainty on the borehole test chamber compressibility (Tremosa et al., 2010). The asterisk refers to the fact that the linear regression (dashed line) is based on the available data excepting the in situ values. Linear analytical theoretical expressions $\varepsilon_T - \varepsilon_T^S = A \times \sigma/b$ are obtained with $A = 2.50 \times 10^{-3}$ and $A = 3.25 \times 10^{-3}$ for clays in Ca and Na solutions, respectively. The gray area represents the uncertainty for clays with Na pore fluid (see equation (22) and related text).

through molecular dynamics simulations. Therefore, using the model to compute $\varepsilon_T = \Delta H/T$ for given petrophysical data (ω, CEC, and A_S) and bulk solution chemical composition (c_b, c_+, c_{2+}) consists first in calculating Q_V using equation (11) and solving equation (12) to obtain C_-, then equations (8) and (9) to obtain C_+ and C_{2+} which are introduced in equations (14) and (15). Calculated C^b_{HB} and C_{HB} values are finally introduced in equation (13) which enables the computation of $\varepsilon_T = \Delta H/T$ for a given T value.

3. Results

3.1. Asymptotic Analysis to Identify Controlling Factors

The analysis presented here is limited to NaCl pore and bulk solutions (c_{2+}=C_{2+}=0) corresponding to the only available data. The previous monovalent version of this model reproduces reasonably these data (see Table S1 in the supporting information) by respecting the sign and the order of magnitude of experimental ε_T values (Gonçalvès et al., 2012, Figure 3). In this case, the Donnan equilibrium model reduces to more trivial expressions; counterions and co-ions in the porosity of the charged porous medium are

$$C_+ = \sqrt{\frac{Q_V^2}{4N_a^2e^2} + c_b^2} + \frac{Q_V}{2N_ae}, C_- = \sqrt{\frac{Q_V^2}{4N_a^2e^2} + c_b^2} - \frac{Q_V}{2N_ae}, \quad (19)$$

where N_a is Avogadro's constant (6.02×10^{23} mol^{-1}). Note that in equation (19), concentrations are in mol m^{-3}. The molecular parameters values from the literature (Di Tommaso et al., 2014; Gonçalvès & Rousseau-Gueutin, 2008; Guàrdia et al., 2005; Hakem et al., 2007; Marry et al., 2008; Zavistas, 2005) used in the model are listed in Table 1. The similar state of hydration of ions in the pore space and in the bulk solution postulated here is supported by molecular dynamics simulations for clay-solution systems (Marry & Turq, 2003). At large values of the surface charge density σ, $C^+ \gg c^+ = c_- = c_b$, $C^+ \gg C^-$, assuming $\frac{b-b_s}{b}N^b_{HB} + \frac{b_s}{b}N^s_{HB} \approx N^b_{HB}$ for the sake of simplicity, the thermo-osmotic coefficient reduces to

$$\varepsilon_T \approx \frac{\Delta H_{HB}}{T} C_+ \left[\left(\frac{\nu_+}{\nu_w} + N_w^+\right)\frac{N^b_{HB}}{2} - \frac{N_w^+ N^+_{HB}}{2} \right]. \quad (20)$$

Consequently, the osmotic coefficient is directly proportional to $C_+ \approx \frac{Q_V}{N_ae}$ and thus to $CEC \times 96.3/A_s b = \sigma/b$ which is expected to be a dominant controlling factor. Conversely, at low surface charge density; that is, when σ tends to zero, ε_T is dominated by the last term in the right-hand side of equation (14) relative to the presence of more structured water at the mineral surface yielding

$$\varepsilon_T \approx \varepsilon_T^S = \frac{\Delta H_{HB}}{2T\nu_w}(N^b_{HB} - N^s_{HB})\frac{b_s}{b}, \quad (21)$$

which corresponds to the limiting case of negative thermo-osmotic coefficients ε_T^S. Based on the controlling factors suggested by the above asymptotic analysis, $\varepsilon_T - \varepsilon_T^S$ can be represented as a function σ/b. Both the available data for clays with Na pore fluid (see Table S1 in the supporting information) and a model curve are depicted in Figure 2 and show clear linear relationships: $\varepsilon_T - \varepsilon_T^S = A \times \sigma/b$. The model curve was obtained by means of multiple (50,000) simulations which were run using randomly selected values of σ, b, and c_b sorted in uniform distributions bonded by 0.05 and 0.6 C m^{-2}, 1 and 200 nm, and 10^{-4} and 1 mol L^{-1}, respectively. Then the best fit of randomly modeled ε_T values for clays with pure Na pore fluid was computed. Introducing plausible and average values for the molecular parameters without any calibration process yields a reasonable agreement between the model and the data. The weak dispersion of the simulated values for clays with Na solutions is illustrated by the low values for the uncertainty on the slope, A=3.25 × 10^{-3} ± 6 × 10^{-7}.

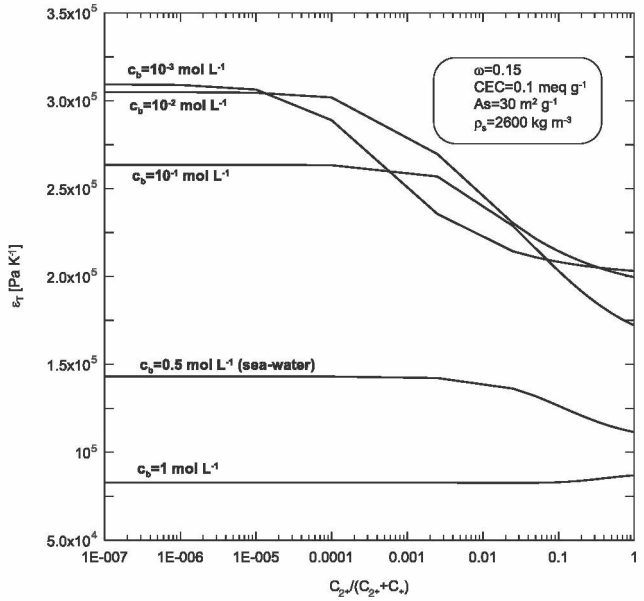

Figure 3. Effect of divalent cations on the thermo-osmotic coefficient at different chlorine concentrations in the bulk solution c_b for a typical natural clay rock whose petrophysical properties are listed in the inset and using the mathematical model of section 2.

Beyond these weak uncertainties, more significant ones associated with the molecular parameters of the model (Table 1) must be analyzed. In the range of natural values, temperature only slightly affects the molecular parameters (Afanasiev et al., 2009; Gonçalvès et al., 2012) unlike ionic concentrations. In NaCl solutions, a 25% decrease of N_w^+ was described (Gallo et al., 2011) with increasing concentration (from nearly pure water to about 4 mol L^{-1} solution), while N_w^-, N_{HB}^+, and N_{HB}^- are almost insensitive to concentration (Nag et al., 2008). The uncertainty on N_{HB}^s and ΔH_{HB} is 0.25 (value between 3.5 and 4) and 8.5 kJ mol^{-1} (between 6 and 23 kJ mol^{-1}), respectively. The error on molecular parameters (σ_{p_i} for parameter p_i) propagates and affects the slope A whose uncertainty is given by

$$\sigma_A^2 = \sum_{i=1}^{N} \left(\frac{\partial A}{\partial p_i} \right)^2 \sigma_{p_i}^2. \tag{22}$$

Using the values for NaCl solutions yields the 61% uncertainty for A illustrated in Figure 2 which is largely dominated by the error on ΔH_{HB}.

3.2. Effect of Divalent Cations

A model curve was obtained for purely clays in calcium solutions (see Figure 2) in the same fashion as for the Na case by multiple random simulations and a subsequent linear regression on simulated ε_T values. The regression is characterized by a weak dispersion of simulated ε_T around the linear model with a slope value $A = 2.50 \times 10^{-3} \pm 4 \times 10^{-7}$ pointing to thermo-osmotic coefficients lower on average by one fourth compared to clays with Na pore fluid. For a given clay, the amount of Ca^{2+} to balance the negative charge of clay particles is half the amount of Na^+, while the molecular parameters describing the cation HB disruption effect (N_{HB}^{2+}, N_w^{2+}) are not twice as high as those for sodium. Therefore, the lower Ca^{2+} concentration is not balanced by molecular parameters values whence the lower disruption effect and ε_T values for calcium solutions. The same uncertainty analysis can be performed for the Ca^{2+} model using uncertainties of 25% and 15% for N_w^{2+} and N_{HB}^{2+}, respectively (Di Tommaso et al., 2014; Zavistas, 2005) and the same uncertainties for the other molecular parameters considered above. A final uncertainty of about 61% is also obtained for slope A applied to clays with Ca solutions.

A more refined analysis is shown in Figure 3, which represents the calculated effect of the divalent proportion $f = c_{2+}/(c_{2+} + c_+)$ in the bulk solution on thermo-osmotic coefficients ε_T for a typical natural clay rock such as the shale formations currently studied for their nuclear waste confinement properties (Gonçalvès et al., 2012, Callovo-Oxfordian Formation, France). Increasing the divalent fraction slightly reduces the thermo-osmotic permeability due to a weakening of the HB network disruption effect of the cations. Therefore, fewer divalent cations are required to balance the negative surface charge of clay minerals while the number of water molecules in the first hydration shell of divalent cations is only slightly higher. Hence, the thermo-osmotic coefficient is reduced at most by about one third in clays with purely divalent solutions (here Ca^{2+}) as compared to clays in monovalent (Na^+) ones for typical values of the chlorine concentrations, that is, $c_b < 0.5$ mol L^{-1}. A more drastic effect of divalent cations was evidenced in the case of chemical osmosis (see below). Figure 3 also shows that only a few percent of divalent cations such as Ca^{2+} are needed in the solution for the thermo-osmotic coefficient ε_T to show the characteristic values for clay rocks with purely divalent pore fluid. This is an important result since divalent cations (Ca^{2+}, Mg^{2+}) are naturally present in shale formations even at low concentration.

4. Discussion and Conclusions

Based on limiting cases analysis (low and large surface charge density), some hitherto lacking analytical theoretical expressions for the thermo-osmotic coefficient are proposed here both for clays in contact with pure Na and Ca solutions:

$$\varepsilon_T = A_{ST} \frac{b_s}{b} + A \frac{\sigma}{b}, \tag{23}$$

where $A_{ST} = \frac{\Delta H_{HB}}{2Tv_w}(N_{HB}^b - N_{HB}^s)$=-3.38 × 10^5 (at T=298 K) and A is 3.25 × 10^{-3} and 2.50 × 10^{-3} for clays containing Na and Ca solutions, respectively. For clay rocks with Na pore fluid, the expression is in fairly good

agreement with the data except for the only available values based on in situ measurements. Interestingly, the monovalent thermo-osmotic model depicted in Figure 2 roughly corresponds to the linear regression based purely on the data with the notable exception of the in situ values acquired by Tremosa et al. (2010) for the Toarcian shale in Tournemire, France. This suggests a possible overestimation by about 1 order of magnitude, which can be explained by the difficult interpretation of an in situ experiment which is far less constrained (in terms of boundary conditions and effective gradients) than experiments on core samples. It should also be mentioned here that the hydraulic conductivity is often known within 1 order of magnitude in such complex natural media (see, e.g., Yu et al., 2017).

In this study, it is shown that the presence of a divalent cation reduces the thermo-osmotic coefficient by at most one third, which is far lower than for chemical osmosis, as discussed by Tremosa et al. (2012). Therefore, these authors showed that increasing the calcium content decreases the chemical osmotic coefficient by a factor of 5 to 10, which in turn reduces the overpressuring (pressures above the hydrostatic or adjacent aquifers' pressures) ability of such a process in shale formations. In natural media, the likely presence, even at a few percent, of divalent cations decreases ε_T almost to its purely divalent value. Consequently, the analytical expression of ε_T for divalent cations is expected to describe better the thermo-osmotic behavior of natural materials. The mathematical formalism derived here is based on (i) plane-parallel geometrical concept for transport processes and (ii) an average macroscopic behavior controlled by "representative pores" (see supporting information). Plane-parallel transport is a fairly good approximation at high compaction state and clay content but at lower compaction state or clay content, alternative microstructures can hold (Fu et al., 2017). For loosely compacted materials or at low clay content, a macroscopic "abacus-type" relation between ε_T and Q_V independent from any geometrical model can be used such as proposed by Gonçalvès et al. (2015). Here the heterogeneity (presence of nonclay grains) of natural materials was simply accounted for by considering an overall microstructure controlled by the plane-parallel geometry presumably imposed by the clay fraction surrounding the nonclay grains (see supporting information). This simplifying assumption allows a convenient extension of equation (16), while a higher complexity for a more rigorous expression describing the microstructure in natural media can be expected. In such natural and thus heterogeneous clay materials, clay interparticle spaces can act as pore throats (see section 1 in the supporting information). If pore throats effect is at work, it is supposed that these small pores control transport processes leading to an overall (macroscopic) membrane behavior of the material caused by the associated electrochemical interactions. However, in case of by-pass circulations through continuous large pores, no membrane properties of the material can be expected. Similarly, to other osmotic expression (e.g., chemical osmosis) simple representative solutions combining Na^+, Ca^{2+}, and Cl^- are considered which is a clear simplification of natural pore solutions. More realistic multi-ionic solutions could be introduced but require a more complex resolution of Donnan equilibrium equations in comparison to our analytical expression. However, provided the similar ionic radius of the for the two dominant divalent cations (Mg^{2+} and Ca^{2+}), the HB disruption effect could be slightly equivalent.

Despite the fairly good agreement between the thermo-osmotic estimates using our simple heuristic model and the available data that supports the theoretical molecular-based background proposed 75 years ago by Derjaguin and coworkers, some molecular dynamics simulations such as those made by Fu et al. (2017) for a pure fluid could increase the confidence in the ability of the theory to describe thermo-osmotic and mechanocaloric effects. In addition, more constrained and thus controlled thermo-osmotic experiments at sample scale for natural clay rocks are still lacking, to the best of our knowledge. This would represent an important contribution to definitively establish the occurrence of such processes for shale formations. Despite all these limitations, the analytical expressions proposed here could be used for safety calculations in the context of deep geological nuclear waste repositories.

Acknowledgments
Financial support from the Mont Terri Project and the French CNRS through the NEEDS program are acknowledged. We gratefully thank the four reviewers for their constructive comments which allowed substantial improvements of the manuscript. The data used in this article are available in Table S1 in the supporting information.

References

Afanasiev, V. N., Ustinov, A. N., & Vashurina, I. Y. (2009). State of hydration shells of sodium chloride in aqueous solutions in a wide concentration range at 273.15–373.15 K. *Journal of Physical Chemistry B, 113*, 212–223.

Al-Bazali, T. M. (2005). Experimental study of the membrane behavior of shale during interaction with water-based and oil-based muds, (PhD thesis). (304 pp.). Austin, TX: University of Texas.

Bennett, R. H., & Hulbert, M. H. (1986). *Clay microstructure*. Boston: IHRDC Press.

Cary, J. W. (1966). Soil moisture transport due to thermal gradients: Practical aspects. *Soil Science Society of America, Proceedings, 30*, 428–433.

Churaev, N. V. (2000). *Liquid and vapour flows in porous bodies: Surface phenomena*. London: Taylor & Francis.

Derjaguin, B. V., & Sidorenkov, G. P. (1941). On thermo-osmosis of liquid in porous glass. *Proceedings of the USSR Academy of Sciences*, *32*, 622–626.

Di Tommaso, D., Ruiz-Agudo, E., de Leeuw, N. H., Putnis, A., & Putnis, C. V. (2014). Modelling the effects of salt solutions on the hydration of calcium ions. *Physical Chemistry Chemical Physics*, *16*, 7772–7785.

Dirksen, C. (1969). Thermo-osmosis through compacted saturated clay membranes. *Soil Science Society of America, Proceedings*, *33*, 821–826.

Fu, L., Merabia, S., & Joly, L. (2017). What controls thermo-osmosis? Molecular simulations show the critical role of interfacial hydrodynamics. *Physical Review Letters*, *119*, 214501.

Gallo, J., Corradini, D., & Rovere, M. (2011). Ion hydration and structural properties of water in aqueous solutions at normal and supercooled conditions: A test of the structure making and breaking concept. *Physical Chemistry Chemical Physics*, *13*, 19,814–19,822.

Gonçalvès, J., & Rousseau-Gueutin, P. (2008). Molecular-scale model for the mass density of electrolyte solutions bound by clay surfaces: Application to bentonites. *Journal of Colloid and Interface Science*, *320*, 590–598.

Gonçalvès, J., & Tremosa, J. (2010). Thermo-osmosis in clay-rocks: I. Theoretical insights. *Journal of Colloid and Interface Science*, *342*, 166–174.

Gonçalvès, J., Adler, P. M., Cosenza, P., Pazdniakou, A., & de Marsily, G. (2015). Semipermeable membrane properties and chemo-mechanical coupling in clay barriers. In C. Tournassat, et al. (Eds.), *Developments in Clay Science, Natural and Engineered Clay Barriers* (Vol. 6, pp. 269–327). Amsterdam, Netherlands: Elsevier.

Gonçalvès, J., de Marsily, G., & Tremosa, J. (2012). Importance of thermo-osmosis for fluid flow and transport in clay fomations hosting a nuclear waste repository. *Earth and Planetary Science Letters*, *339-340*, 1–10.

Gray, D. H. (1966). Coupled flow in clay-water systems (PhD thesis). (170 pp.). Berkeley, CA: University of California.

Guàrdia, E., Martí, J., García-Tarrés, L., & Laria, D. A. (2005). Molecular dynamics simulation study of hydrogen bonding in aqueous ionic solutions. *Journal of Molecular Liquids*, *117*, 63–67.

Habib, . P., & Soeiro, F. (1957). Water movement in soils promoted by a thermal gradient. In *Proceedings of the 4th International Congress on Soil Mechanics* (pp. 40–43).

Hakem, I. F., Boussaid, A., Benchouk-Taleb, H., & Bockstaller, M. R. (2007). Temperature, pressure, and isotope effects on the structure and properties of liquid water: A lattice approach. *Journal of Chemical Physics*, *127*(22), 224106.

Kirkpatrick, R. J., Kalinichev, A. G., & Wang, J. (2005). Molecular dynamics modelling of hydrated mineral interlayers and surfaces: Structure and dynamics. *Mineralogical Magazine*, *69*, 287–306.

Leu, L., Georgiadis, A., Blunt, M. J., Busch, A., Bertier, P., Schweinanr, K., … Ott, H. (2016). Multiscale description of shale pore system by scanning SAXS and WAXS microscopy. *Energy Fuels*, *30*, 10282–10297.

Marry, V., & Turq, P. (2003). Microscopic simulations of interlayer structure and dynamics in bihydrated heteroionic montmorillonites. *Journal of Physical Chemistry B*, *107*, 1832–1839.

Marry, V., Rotenberg, M., & Turq, P. (2008). Structure and dynamics of water at a clay surface from molecular dynamics simulation. *Physical Chemistry Chemical Physics*, *10*, 4802–4813.

Mitchell, J. K. (1993). *Fundamentals of soil behavior*. New York: John Wiley.

Nag, A., Chakraborty, D., & Chandra, A. (2008). Effects of ion concentration on the hydrogen bonded structure of water in the vicinity of ions in aqueous NaCl solutions. *Journal of Chemical Sciences*, *120*, 71–77.

Neuzil, C. E. (2000). Osmotic generation of "anomalous" fluid pressures in geological environments. *Nature*, *403*, 182–184.

Neuzil, C. E., & Provost, A. M. (2009). Recent experimental data may point to a greater role for osmotic pressures in the subsurface. *Water Resources Research*, *45*, W03410. https://doi.org/10.1029/2007WR006450

Revil, A., & Leroy, P. (2004). Constitutive equations for ionic transport in porous shales. *Journal of Geophysical Research*, *109*, B03208. https://doi.org/10.1029/2003JB002755.6

Revil, A., & Pessel, M. (2002). Electroosmotic flow and the validity of the classical Darcy equation in silty shales. *Geophysical Research Letters*, *29*(9), 1300. https://doi.org/10.1029/2001GL013480

Rosanne, M., Paszkuta, M., & Adler, P. M. (2006). Electrokinetic phenomena in satured compact clays. *Journal of Colloid and Interface Science*, *297*, 353–364.

Sposito, G., Skipper, N. T., Sutton, R., Park, S.-H, Soper, A. K., & Greathouse, J. A. (1999). Surface geochemistry of the clay minerals. *Proceedings of the National Academy of Sciences of the United States of America*, *96*, 3358–3364.

Taylor, S. A., & Cary, J. W. (1960). Analysis of the simultaneous flow of water and heat or electricity with the thermodynamics of irreversible processes. In *Transactions of the 7th International Congress of Soil Science* (Vol. I, pp. 80–90). Madison, WI.

Tremosa, J., Gonçalvès, J., & Matray, J.-M. (2012). Natural conditions for more limited osmotic abnormal fluid pressures in sedimentary basins. *Water Resources Research*, *48*, W04530. https://doi.org/10.1029/2011WR010914

Tremosa, J., Gonçalvès, J., Matray, J.-M., & Violette, S. (2010). Thermo-osmosis in clay-rocks: II. In-situ experimental approach. *Journal of Colloid and Interface Science*, *342*, 175–184.

Wenk, H.-R., Voltolini, M., Mazurek, M., Van Loon, L. R., & Vinsot, A. (2008). Preferred orientations and anisotropy in shales: Callovo-oxfordian shale (France) and Opalinus Clay (Switzeland). *Clays and Clay Minerals*, *56*, 285–306.

Yu, C., Matray, J.-M., Gonçalvès, J., Jaeggi, D., Grasle, W., Wieczorek, K., … Sykes, E. (2017). Comparative study of methods to estimate hydraulic parameters in the hydraulically undisturbed Opalinus Clay (Switzerland). *Swiss Journal of Geosciences*, *110*(1), 85–104. https://doi.org/10.1007/s00015-016-0257-9

Zavistas, J. (2005). Aqueous solutions of calcium ions: Hydration numbers and the effect of temperature. *Journal of Physical Chemistry B*, *109*, 20636–20640. https://doi.org/10.1021/jp053909i

Zheng, L., & Samper, J. (2008). A coupled THMC model of FEBEX Mock-up test. *Physics and Chemistry of the Earth*, *33*, S486–S498.

Zhang, L., & Wang, M. (2017). Electro-osmosis in inhomogeneously charged microporous media by pore-scale modeling. *Journal of Colloid and Interface Science*, *486*, 219–231.